Magnesium Technology 2011
Edited by: Wim H. Sillekens, Sean R. Agnew, Neale R. Neelameggham, and Suveen N. Mathaudhu
TMS (The Minerals, Metals & Materials Society), 2011

OPTIMIZATION OF MAGNESIUM-ALUMINUM-TIN ALLOYS FOR AS-CAST MICROSTRUCTURE AND MECHANICAL PROPERTIES

Xiaoyu Kang[1], Alan A. Luo[2], Penghuai Fu[1], Zhenzhen Li[1], Tianyu Zhu[1], Liming Peng[1], Wenjiang Ding[1]
[1] National Engineering Research Center of Light Alloys Net Forming and State Key Laboratory of Metal Matrix Composites, Shanghai Jiao Tong University, 200030, Shanghai, P. R. China
[2] General Motors Global Research & Development, Warren, MI, 48090, USA

Keywords: magnesium alloy development, mechanical properties, microstructure, computational material design.

Abstract

The microstructure and mechanical properties of as-cast Mg–Al-Sn alloys have been investigated using computational alloy design and experimental approaches. The as-cast microstructure of Mg-Al-Sn alloys consists of α-Mg, $Mg_{17}Al_{12}$ and Mg_2Sn phases. The volume fractions of $Mg_{17}Al_{12}$ and Mg_2Sn phases increase with increasing Al/Sn contents, and show good agreement between computational thermodynamics modeling and the experimental results. Generally, the yield strength of as-cast alloys increases with Al/Sn alloying contents, while the ductility decreases. This study has confirmed an earlier development of Mg-7Al-2Sn alloy and led to a promising new Mg-7Al-5Sn alloy with significantly improved strength and ductility compared to commercial alloy AZ91 (Mg-9Al-1Zn).

Introduction

The low density of magnesium alloys makes them an attractive material for lightweight components in the automotive industry. There are three main alloy systems in magnesium alloy applications: Mg-Al, Mg-Zn and Mg-RE based alloys. Mg-RE based alloys have the best mechanical properties among these three alloy systems, but their costs are generally too high for high-volume automotive applications. Mg-Zn based alloys are usually used as wrought alloys due to their poor castability, such as the tendency for hot tearing during casting. The most widely used Mg alloys are Mg-Al based alloys [1], as Al improves the castability and mechanical properties at room temperature. Currently, the application of commercially available Mg-Al based alloys is limited to room- or near room-temperature applications due to their poor creep resistance at elevated temperatures. This is mainly caused by the grain boundary $Mg_{17}Al_{12}$ phase, which softens at temperatures exceeding 120°C [2]. Additions of Sn to Mg-Al alloys were found to improve the strength [3] and creep-resistance [4, 5] of the alloys. Also, the Mg-Sn system is known as an age-hardening alloy system due to the precipitation of Mg_2Sn, a face-centered cubic (fcc) phase with a high melting temperature of 770°C [6]. Despite those interesting findings, there has been no systematic investigation and composition optimization of Mg-Al-Sn system for microstructure and resultant mechanical properties.

In the present study, the microstructure and mechanical properties of as-cast Mg-Al-Sn alloys have been investigated using a computational alloy design approach supported by experimental results. While the binary phase diagrams of Mg-Sn, Al-Sn and Mg-Al systems are well established [7-9], the thermodynamic data of the Mg-Al-Sn system was only made available recently [10]. Therefore, thermodynamic calculations of Mg-Al-Sn system were carried out using a software package Pandat developed by CompuTherm, Madison, WI [11]. The calculated phase diagrams, phase constituents, and solidification paths were then used to design the alloy compositions with balanced mechanical properties.

Thermodynamic Calculations and Alloy Design

Phase Constituents and Alloy Design

Fig. 1 shows the calculated liquidus projection of the Mg-Al-Sn system in the Mg-rich corner. No ternary stable phase was discovered, and no ternary solubilities of the binary intermetallic phases were found in this calculation, which is consistent with a previous study [10]. Two binary phases, Mg_2Sn and $Mg_{17}Al_{12}$, are important to this alloy system. Mg_2Sn phase is reportedly to provide significant strengthening [3], while $Mg_{17}Al_{12}$ phase improves strength [12], corrosion and castability [13], but reduces ductility and creep resistance [2]. In designing the new Mg-Al-Sn alloys for automotive structural applications, mechanical properties and corrosion resistance are primary considerations. Fig. 1 suggests that the equilibrium phase constituents (Mg_2Sn and $Mg_{17}Al_{12}$) of Mg-Al-Sn alloys are determined by the Al and Sn contents. Table 1 lists the nominal compositions of the experimental alloys studied in this investigation, along with a baseline alloy AZ91.

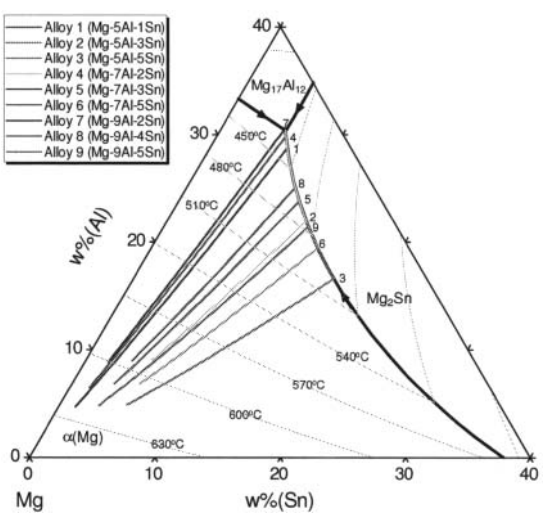

Fig. 1. Calculated Mg-Al-Sn liquidus projection and the solidification paths of the experimental alloys.

Table 1. Chemical compositions (in wt.%) of experimental Mg-Al-Sn alloys and commercial AZ91 alloy

Alloy #	Nominal composition	Al	Sn	Zn	Mg
1	Mg-5Al-1Sn	4.67	1.32	-	Bal.
2	Mg-5Al-3Sn	4.77	3.13	-	Bal.
3	Mg-5Al-5Sn	4.82	5.33	-	Bal.
4	Mg-7Al-2Sn	6.64	1.54	-	Bal.
5	Mg-7Al-3Sn	6.83	3.34	-	Bal.
6	Mg-7Al-5Sn	6.81	5.37	-	Bal.
7	Mg-9Al-2Sn	8.84	1.85	-	Bal.
8	Mg-9Al-4Sn	8.95	3.70	-	Bal.
9	Mg-9Al-5Sn	9.01	5.26	-	Bal.
AZ91	Mg-9Al-1Zn	9.14	-	1.33	Bal.

Scheil Simulation Results

Based on the assumption of complete mixing in the liquid but no diffusion in the solid, Scheil solidification model available in the Pandat package is much closer to the actual casting conditions compared to the equilibrium model based on infinite diffusion in both liquid and solid states. The solidification paths of the nine experimental Mg-Al-Sn alloys are also shown in Fig. 1, and they were calculated using the Scheil model. Table 2 summarizes the Scheil simulation results of the experimental Mg-Al-Sn alloys using Pandat, including the volume fractions of Mg_2Sn and $Mg_{17}Al_{12}$ phases in the alloys, as well as the liquidus and solidus temperatures. The simulation results suggest the following solidification sequence for the alloys upon cooling:

(1) Nucleation of primary magnesium (from liquidus):
$L \rightarrow L + \alpha\text{-Mg}$
(2) Binary eutectic reaction (439°C):
$L \rightarrow L + \alpha\text{-Mg} + Mg_2Sn$
(3) Ternary eutectic reaction (430°C):
$L \rightarrow L + \alpha\text{-Mg} + Mg_2Sn + Mg_{17}Al_{12}$

Table 2. Scheil simulation results of experimental Mg-Al-Sn alloys using Pandat

Alloy #	Nominal composition	Mg_2Sn, vol. %	$Mg_{17}Al_{12}$, vol. %	Liquidus, °C	Solidus, °C
1	Mg-5Al-1Sn	0.24	4.00	610	430
2	Mg-5Al-3Sn	0.72	4.38	606	430
3	Mg-5Al-5Sn	1.47	4.65	602	430
4	Mg-7Al-2Sn	0.33	6.46	605	430
5	Mg-7Al-3Sn	0.88	7.27	600	430
6	Mg-7Al-5Sn	1.62	7.64	596	430
7	Mg-9Al-2Sn	0.45	10.32	599	430
8	Mg-9Al-4Sn	1.08	10.82	595	430
9	Mg-9Al-5Sn	1.72	11.12	590	430

The nucleation of primary magnesium (α-Mg) starts from the liquidus temperature (610-590°C as shown in Table 2), and its volume fraction increases until the melt reaches the binary eutectic temperature of 439°C when Mg_2Sn phase is formed as part of the (α-Mg + Mg_2Sn) eutectic structure. Furthermore, $Mg_{17}Al_{12}$ is formed at 430°C as result of the ternary eutectic reaction (α-Mg + Mg_2Sn + $Mg_{17}Al_{12}$), which completes the solidification at this temperature (solidus in Table 2).

Experimental Procedures

Materials and Casting

The experimental alloys listed in Table 1 were prepared by melting high-purity Mg, Al and Sn ingots in an electrical resistance furnace under the protection of mixture gas of SF_6, CO_2 and air, and then cast into a permanent mold at a pouring temperature of 710±5°C and mold temperature of 150±5°C. Commercial alloy AZ91 (Mg-9Al-1Zn) was also prepared and cast in the same conditions for comparison. The actual chemical compositions of the alloys were analyzed using inductively coupled plasma analyzer (ICP) technique and the results are also listed in Table 1.

Microstructural Analysis and Mechanical Testing

Specimens for microstructural analysis were etched in a 4 vol.% nital or in a solution of 20 ml acetic acid + 60 ml ethanol + 1 ml nitric acid + 19 ml water. Microstructure was examined using an optical microscope (OM) and a JSM-6460 scanning electron microscope (SEM). The identification of various secondary phases was carried out using a D/MAX-IIIA X-ray diffractometer (XRD). Quantitative image analysis technique was used to measure the area fractions of secondary phases from the SEM images of the as-cast alloys. Since the optical images do not clearly reveal grain boundaries, the average grain sizes of the alloys were measured from the solution-treated (16 h at 420°C) samples, using a linear intercept method.

Tensile test samples were cut into flat tensile specimens with dimensions of 3.5 mm width, 2 mm thickness and 10 mm gage length using an electric-sparking wire-cutting machine. Tensile testing was carried out on a Zwick/Roell-20 kN material test machine at a cross head speed of 1 mm/min at room temperature. Three tensile samples were tested for each alloy. Fracture surfaces of the tensile test samples were investigated using an SEM.

Experimental Results and Discussion

Microstructure

Fig. 2 shows the SEM images of as-cast microstructure of Mg-Al-Sn alloys, all of which is comprised of dendrites of magnesium matrix surrounded by eutectic compounds. With increasing Al and/or Sn contents, the volume fractions of the eutectic compounds increase. The XRD patterns in Fig. 3 confirm the two compounds of $Mg_{17}Al_{12}$ and Mg_2Sn in the as-cast microstructure as calculated in this study. The two eutectic phases have different morphology in the SEM images, as shown in Fig. 4(a) which is the as-cast microstructure of the Mg-9Al-5Sn alloy, compared to that of AZ91 alloy, Fig. 4(b). The quantitative EDS analysis results of the different phases in Fig. 4(a) are shown in Table 3. Point A in Fig. 4(a) contains Mg and Al, with the composition ranges indicating the $Mg_{17}Al_{12}$ phase; while Point B contains Mg and Sn, suggesting the Mg_2Sn phase. Table 4 compares the measured area fractions and the calculated volume fractions of $Mg_{17}Al_{12}$ and Mg_2Sn phases in the Mg-Al-Sn alloys, and shows a reasonable agreement between the measurements and the Scheil simulation results.

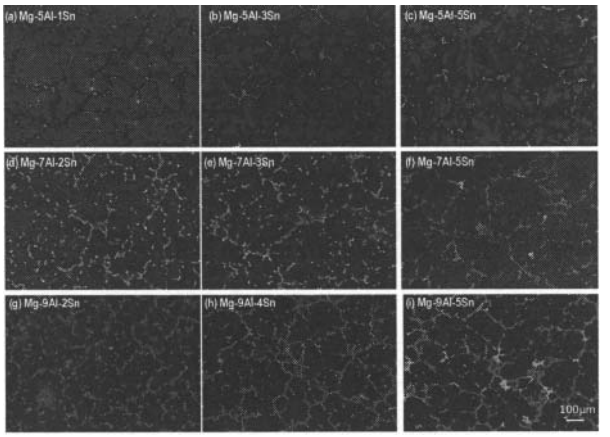

Fig. 2. SEM micrographs showing the as-cast microstructure of Mg-Al-Sn alloys.

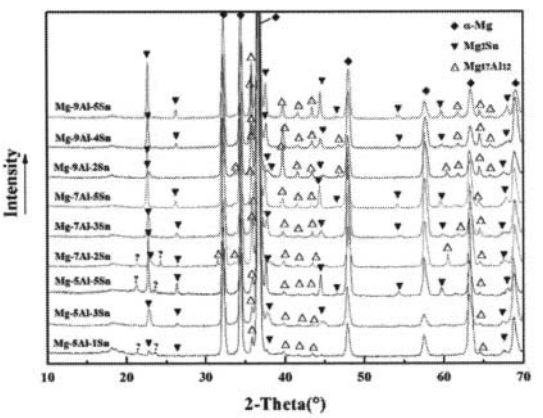

Fig. 3. XRD patterns of as-cast Mg-Al-Sn alloys.

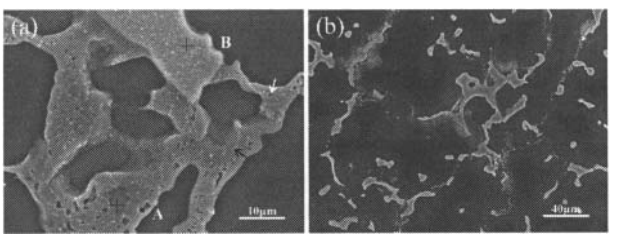

Fig. 4. SEM micrographs showing the as-cast microstructure of (a) Mg-9Al-5Sn alloy; and (b) AZ91 (Mg-9Al-1Zn) alloy.

Table 3. Quantitative EDS analysis results of Point A and Point B in Fig. 4(a)

Element (at.%)	Mg	Al	Sn
Point A	69.96	29.29	00.75
Point B	65.90	04.51	29.59

Fig. 5 shows the grain structure of solution-treated (16 h at 420°C) Mg-Al-Sn alloys. The grain sizes of Mg-Al-Sn alloys are summarized in Table 4. Generally, with increasing Al and/or Sn contents, the average grain size decreases due to the fact that more eutectic structures form during solidification and restrict the growth of α-Mg grains. However, Mg-5Al-3Sn and Mg-9Al-4Sn alloys have slightly finer grains compared to Mg-5Al-5Sn and Mg-9Al-5Sn alloys, respectively. The Mg-5Al-1Sn alloy has the coarsest grains, as shown in Fig. 5(a), about 300 μm, and the average grain size decreases to about 150 μm when the Al content is increased from 5% to 7% or the Sn content from 2% to 4%. Further increases of Al and/or Sn contents lead to finer grains, and the Mg-9Al-4Sn alloy has the finest average grain size of about 74 μm. Compared to the AZ91 alloy, with an average grain size of about 180 μm, all Mg-Al-Sn alloys but the Mg-5Al-1Sn alloy have finer grains (Table 4).

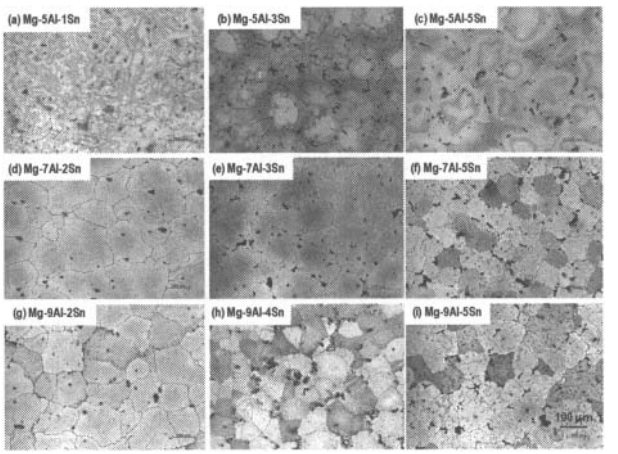

Fig. 5. Optical micrographs showing the grain structure of solution-treated (16 h at 420°C) Mg-Al-Sn alloys.

Table 4. The average grain sizes and second phase contents of Mg-Al-Sn alloys

Alloy	Average grain size (μm)	$Mg_{17}Al_{12}$		Mg_2Sn	
		Calculated (volume %)	Measured (area %)	Calculated (volume %)	Measured (area %)
Mg-5Al-1Sn	295	4.00	3.62	0.24	0.18
Mg-5Al-3Sn	149	4.38	4.36	0.72	1.06
Mg-5Al-5Sn	135	4.65	4.60	1.47	1.49
Mg-7Al-2Sn	147	6.46	6.22	0.33	0.41
Mg-7Al-3Sn	121	7.27	6.79	0.88	0.98
Mg-7Al-5Sn	81	7.64	7.04	1.62	2.07
Mg-9Al-2Sn	119	10.32	11.57	0.45	0.55
Mg-9Al-4Sn	74	10.82	11.30	1.08	1.17
Mg-9Al-5Sn	91	11.12	11.46	1.72	1.84

Tensile Properties

Table 5 lists the tensile properties of as-cast Mg-Al-Sn alloys at room temperature. With increasing Al and/or Sn contents, the yield strength (YS) of the alloys generally increase; while the ultimate tensile strength (UTS) and elongation decrease. Compared to the commercial AZ91 alloy, the properties of Mg-Al-Sn alloys are summarized as follows:

(1) Mg-7Al-2Sn and Mg-7Al-5Sn alloys have better mechanical properties (strength and ductility);
(2) Mg-7Al-3Sn alloy has similar properties;

(3) Mg-5Al-1Sn, Mg-5Al-3Sn and Mg-5Al-5Sn alloys have better UTS and elongation but lower YS; and
(4) Mg-9Al-2Sn, Mg-9Al-4Sn and Mg-9Al-5Sn alloys have better YS but lower UTS and elongation.

Table 5. Tensile properties of Mg-Al-Sn alloys

Alloy	Yield strength (MPa)	Ultimate tensile strength (MPa)	Elongation (%)
Mg-5Al-1Sn	64.7±1.4	179.1±17.0	8.32±0.78
Mg-5Al-3Sn	75.7±3.0	177.5±9.9	7.49±2.19
Mg-5Al-5Sn	82.5±4.0	161.1±5.6	4.88±0.72
Mg-7Al-2Sn	***91.9±2.1***	***175.5±6.2***	***5.34±1.04***
Mg-7Al-3Sn	88.8±3.6	151.5±2.7	3.11±0.24
Mg-7Al-5Sn	***110.1±10.1***	***160.7±5.5***	***3.18±0.64***
Mg-9Al-2Sn	102.5±3.3	154.8±2.0	2.05±0.20
Mg-9Al-4Sn	120.4±6.9	160.1±7.0	1.46±0.11
Mg-9Al-5Sn	127±1.3	149.8±2.1	1.08±0.49
AZ91 (Mg-9Al-1Zn)	89.3±4.4	150.8±11.6	2.37±0.49

The results in Tables 4 and 5 suggest that the yield strength of the Mg-Al-Sn alloys increases with increasing alloying elements (Al and Sn), due to the increased volume fraction of the eutectic compounds and the reduced grain size in the microstructure. On the other hand, the ductility (elongation) of the alloys decreases with increasing alloying contents, likely due to the brittleness of the $Mg_{17}Al_{12}$ and Mg_2Sn intermetallic phases [3]. The UTS of alloys is generally a function of YS and elongation, supposedly increasing with yield strength but restrained by the elongation. Therefore, the UTS of the Mg-Al-Sn alloys do not show a clear trend with the alloy compositions in this study.

Fig. 6 is the SEM fractographs of the Mg-Al-Sn alloy tensile specimens. These fracture surfaces show two types of features, the cleavage planes indicating brittle facture in samples of Mg-5Al-1Sn, Mg-5Al-3Sn and Mg-7Al-2Sn alloys; and the ruptured eutectics in all the fracture samples. Cleavage planes generally lead to transgranular fractures as shown in Fig. 6 (b) and (d). All samples show a mixture of intergranular and transgranular fractures. With increasing Al/Sn contents, the samples have more intergranular fractures resulting from the ruptured eutectics, which is evident in all fracture surfaces.

Alloy Optimization

Thermodynamic calculations of Mg-Al-Sn alloy system suggest two binary intermetallic phases $Mg_{17}Al_{12}$ and Mg_2Sn, whose volume fractions in the composition ranges investigated in this study would provide strengthening. The strengthening effects of $Mg_{17}Al_{12}$ and Mg_2Sn have been previously reported [3, 12], and confirmed in this paper. The liquidus and solidus temperatures of the Mg-Al-Sn alloys (Table 2) are similar to those of AZ91 alloy (600°C and 435°C, respectively [14]), indicating possible good castability, which will be verified in future work. Generally, the yield strength of as-cast alloys increases with the Al/Sn contents, while the ductility decreases. Among the alloys studied, the following two alloys show improved mechanical properties compared to AZ91 alloy.

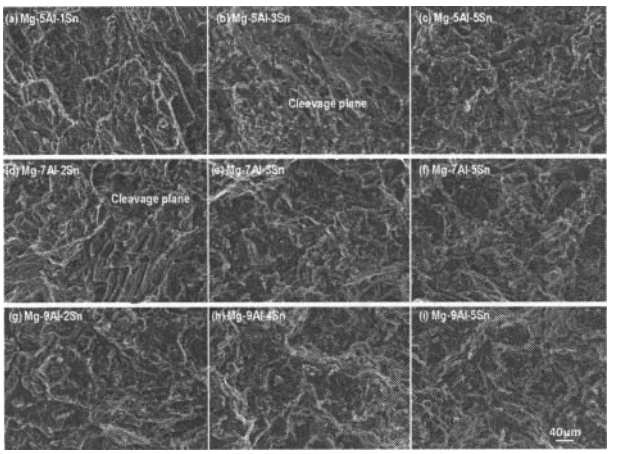

Fig. 6. SEM fractographs showing the fracture surfaces of tensile specimens of Mg-Al-Sn alloys.

(1) The Mg-7Al-2Sn alloy has similar YS, but significant higher UTS (175.5 MPa, 16% increase) and elongation (5.34%, 1.25 times); and
(2) The Mg-7Al-5Sn alloy shows improvements YS (110.1 MPa, 23% increase), UTS (160.7 MPa, 7% increase) and elongation (3.18%, 34% increase)

The identification of Mg-7Al-2Sn alloy in this study confirms the earlier development of AT72 alloy of the same composition for structural applications [3], a high-ductility alloy with similar strength as the AZ91 alloy. It is also promising that the Mg-7Al-5Sn alloy can be developed as a high-strength alloy also with improved ductility. These alloys are presently being studied for die-castability, heat treatment and corrosion resistance.

Conclusions

1. The computational thermodynamic study and experimental investigation of Mg-Al-Sn alloy system have confirmed an earlier development of Mg-7Al-2Sn alloy and led to a promising new Mg-7Al-5Sn alloy with significantly improved strength and ductility compared to commercial AZ91 alloy.

2. The Mg-Al-Sn alloys consist of α-Mg, $Mg_{17}Al_{12}$ and Mg_2Sn phases in the as-cast microstructure, as predicted by computational thermodynamic modeling and experimental validation. The volume fractions of $Mg_{17}Al_{12}$ and Mg_2Sn phases increase with the Al and Sn contents, and show good agreement between the thermodynamic calculations using Scheil solidification model and the experimental measurements.

3. The grain size of as-cast Mg-Al-Sn alloys generally decreases with increasing Al and Sn alloying contents due to the formation of more eutectic structures, restricting the growth of α-Mg grains during solidification. Generally, the yield strength of as-cast Mg-Al-Sn alloys increases with alloying contents, while the ductility decreases, due to the increased volume fractions of the eutectic compounds and the reduced grain size in the microstructure.

Acknowledgments

This work was carried out as a collaborative research project supported by General Motors Global Research and Development (GM R&D), Warren, MI, USA, and Shanghai Jiao Tong University (SJTU), Shanghai, China. Dr. Anil Sachdev of GM R&D and Prof. Xiaoqin Zeng of SJTU are gratefully acknowledged for technical discussions.

References

1. B.L. Mordike, T. Ebert, "Magnesium: Properties-Applications-Potential", Mater. Sci. Eng. A 302 (2001), 37-45.
2. A.A. Luo, "Recent Magnesium Alloy Development for Elevated Temperature Applications", Int. Mater. Rev., 49 (2004), 13-30.
3. A.A. Luo and A.K. Sachdev, "Microstructure and Mechanical Properties of Mg-Al-Mn and Mg-Al-Sn Alloys", in: Magnesium Technology 2009, edited by E.A. Nyberg, S.R. Agnew, N.R. Neelameggham and M.O. Pekguleryuz, TMS, 2009, 437-443.
4. C.L. Mendis, C.J. Bettles, M.A. Gibson, C.R. Hutchinson, "An Enhanced Age Hardening Response in Mg-Sn Based Alloys Containing Zn", Mater. Sci. Eng. A 435-436 (2006), 163-171.
5. S. Avraham, A. Katsman, M. Bamberger, "Strengthening Mechanisms in Mg-Al-Sn Based Alloys", in: Magnesium Technology 2009, edited by E.A. Nyberg, S.R. Agnew, N.R. Neelameggham and M.O. Pekguleryuz, TMS, 2009, 471-475.
6. H. Liu, Y. Chen, Y. Tang, S. Wei, G. Niu, "The Microstructure, Tensile Properties, and Creep Behavior of As-cast Mg-(1-10)%Sn Alloys", J. Alloy Compd. 440 (2007), 122-126.
7. T.B. Massalski, Binary Alloy Phase Diagrams, ASM International, 1990.
8. S.G. Fries and H.L. Lukas, "Optimization of the Mg-Sn System", J Chem. Phys., 90 (1993), 181-187.
9. P. Liang, H.-L. Su, P. Donnadieu, M.G. Harmelin, A. Quivy, P. Ochin, G. Effenberg, H.J. Seifert, H.L. Lukas, and F. Aldinger, "Experimental Investigation and Thermodynamic Calculation of the Central Part of the Mg-Al Phase Diagram", Z. Metallkde., 89 (8) (1998), 536-540.
10. E. Doernberg, A. Kozlov and R. Schmid-Fetzer, "Experimental Investigation and Thermodynamic Calculation of Mg-Al-Sn Phase Equilibria and Solidification Microstructures", Journal of Phase Equilibria and Diffusion, 28 (2007), 523-535.
11. CompuTherm LLC, "Pandat 8.0 - Phase Diagram Calculation Software for Multi-component Systems", CompuTherm LLC, Madison, WI, 53719, USA, 2008.
12. A.A. Luo and A.K. Sachdev: "Microstructure and Mechanical Properties of Magnesium-Aluminum-Manganese Cast Alloys", International Journal of Metalcasting, 4 (4) (2010), 51-58.
13. D. Sachdeva, S. Tiwari, S. Sundarraj and A.A. Luo, "Microstructure and Corrosion Characterization of Squeeze Cast AM50 Magnesium Alloys", Metallurgical and Materials Transactions B, DOI: 10.1007/s11663-010-9433-x.
14. A. Luo, "Understanding the Solidification of Magnesium Alloys" in Proc. of the Third International Magnesium Conference, Ed., G.W. Lorimer, The Institute of Materials, London, UK, 1996, 449-464.